Published in final edited form as:
Nat Neurosci. 2014 April ; 17(4): 540–548. doi:10.1038/nn.3652.

Opioids induce dissociable forms of long-term depression of excitatory inputs to the dorsal striatum

Brady K Atwood, **David A Kupferschmidt**, and **David M Lovinger**
Section on Synaptic Pharmacology, Laboratory for Integrative Neuroscience, National Institute on Alcohol Abuse and Alcoholism, US National Institutes of Health, Bethesda, Maryland, USA

Abstract

As prescription opioid analgesic abuse rates rise, so does the need to understand the long-term effects of opioid exposure on brain function. The dorsal striatum is an important site for drug-induced neuronal plasticity. We found that exogenously applied and endogenously released opioids induced long-term depression (OP-LTD) of excitatory inputs to the dorsal striatum in mice and rats. Mu and delta OP-LTD, although both being presynaptically expressed, were dissociable in that they summated, differentially occluded endocannabinoid-LTD and inhibited different striatal inputs. Kappa OP-LTD showed a unique subregional expression in striatum. A single *in vivo* exposure to the opioid analgesic oxycodone disrupted mu OP-LTD and endocannabinoid-LTD, but not delta or kappa OP-LTD. These data reveal previously unknown opioid-mediated forms of long-term striatal plasticity that are differentially affected by opioid analgesic exposure and are likely important mediators of striatum-dependent learning and behavior.

Opioid analgesics are ubiquitous in modern medicine, and the non-medical use and abuse of prescription opioids are becoming increasingly prevalent[1–4]. Thus, a mechanistic understanding of the long-term effects of opioid exposure on brain function is critical. Mu (MOPr), delta (DOPr) and kappa (KOPr) G protein–coupled opioid receptors are abundantly expressed throughout the CNS[5], as are their endogenous peptide ligands (the enkephalins, endorphins and dynorphins)[6,7], and the peptidases responsible for terminating the actions of these ligands[8–10]. Acting on central opioid receptors, opioid analgesics can markedly modify neurotransmission and alter endogenous forms of synaptic plasticity, including long-term potentiation and LTD[11–13]. Moreover, endogenous opioid peptides have recently been shown to induce long-term plasticity in the hypothalamus and hippocampus[14–17]. Given the

Correspondence should be addressed to: D.M.L. (lovindav@mail.nih.gov).

AUTHOR CONTRIBUTIONS
B.K.A. planned experiments, conducted whole-cell recordings, injections and stereotaxic surgeries, analyzed data, and wrote the manuscript. D.A.K. conducted extracellular field recordings and wrote the manuscript. D.M.L. supervised and assisted in experimental planning and wrote the manuscript.

COMPETING FINANCIAL INTERESTS
The authors declare no competing financial interests.

Note: Any Supplementary Information and Source Data files are available in the online version of the paper.

widespread central expression of the endogenous opioid system, opioid-mediated long-term plasticity may exist in many brain regions.

The endogenous opioid system is prominent in the dorsal striatum, the major input nucleus of the basal ganglia. Glutamatergic inputs to the dorsal striatum arise from sensorimotor and association cortices and thalamic nuclei[18–20] and synapse onto GABAergic medium spiny neurons (MSNs), the principal projection neurons of the striatum[21]. Exogenous opioid agonists[22,23] and endogenous opioid peptides, released following antidromic activation of MSNs by stimulation of the globus pallidus[24], suppress glutamatergic transmission onto MSNs, likely via presynaptic opioid receptors. However, no work to date has found evidence of long-lasting, opioid-mediated plasticity in the striatum. We explored the ability of exogenous and endogenous opioids to induce long-term synaptic plasticity of excitatory transmission in the dorsal striatum. We further probed the effects of acute *in vivo* exposure to the opioid analgesic oxycodone on striatal opioid-mediated plasticity and, by optogenetically targeting cortical and thalamic inputs to the dorsal striatum, asked whether this plasticity is input specific.

RESULTS

Opioid receptor activation produces LTD in dorsal striatum

Bath application of the MOPr agonist DAMGO induced a long-lasting reduction of electrically evoked excitatory postsynaptic current (eEPSC) amplitude in MSNs in the dorsolateral striatum (DLS, 64.6 ± 5.9%, data are presented as mean ± s.e.m. % of baseline; Fig. 1a). We termed this effect mu opioid peptide long-term depression (mOP-LTD), as the selective MOPr antagonist CTAP prevented synaptic depression when applied throughout the recording (93.9 ± 6.0%; Fig. 1b), but did not reverse the depression when applied after cessation of DAMGO application (58.7 ± 5.1%). DAMGO also reduced net striatal output, as measured by population spike amplitude in extracellular field recordings in the DLS (Supplementary Fig. 1a). The DOPr agonist DPDPE similarly induced OP-LTD (dOP-LTD) of eEPSC amplitude in DLS MSNs (73.6 ± 2.8%; Fig. 1c). The selective DOPr antagonist naltrindole (NTI) blocked DPDPE-induced depression (90.2 ± 5.8%; Fig. 1d), but did not reverse established depression (63.6 ± 2.1). DPDPE also reduced population spike amplitude in extracellular field recordings (Supplementary Fig. 1b). Despite prior evidence that KOPr-mediated inhibition of excitatory transmission does not occur in dorsal striatum[22], the KOPr agonist U69,593 produced LTD of eEPSCs in the DLS (77.6 ± 2.8%; Fig. 1e). Nor-BNI, a KOPr antagonist, blocked (91.2 ± 3.4%; Fig. 1f), but did not reverse, this effect (74.7 ± 6.0%). U69,593 also induced LTD in field potential recordings (Supplementary Fig. 1c). OP-LTD induced by each agonist in the DLS was robust at two holding potentials −60 and −80 mV) observed under physiological conditions in striatal MSNs[25] (Supplementary Fig. 2). DAMGO and DPDPE induced LTD of excitatory transmission to the same extent in MSNs in the dorsomedial striatum (DMS) as in DLS MSNs (Supplementary Fig. 2a,b). In contrast, U69,593 had little to no effect in the DMS (Supplementary Fig. 2c), indicating that kOP-LTD is uniquely subregion specific.

Multiple forms of excitatory LTD in the dorsal striatum are expressed as presynaptic inhibition of glutamate release[26,27]. To assess the synaptic site of OP-LTD expression, we

examined the effects of opioid receptor agonists on the ratio of synaptic responses to paired pulses (50-ms interval), a measure that changes reliably with release probability. Both DAMGO and DPDPE induced a prolonged increase in the mean paired-pulse ratio (PPR; DAMGO, 0.99 ± 0.09 to 1.18 ± 0.11; DPDPE, 1.09 ± 0.06 to 1.19 ± 0.06; Fig. 1g,h), indicative of a persistent reduction in glutamate release probability. U69,593 induced a slower onset increase in PPR (1.08 ± 0.07 to 1.19 ± 0.08; Fig. 1i). To further assess the site of OP-LTD expression, we tested the effects of opioid agonists on the frequency and amplitude of spontaneous EPSCs (sEPSCs). DAMGO (Supplementary Fig. 3a–d) and DPDPE (Supplementary Fig. 3e–h) induced prolonged increases in sEPSC inter-event interval (IEI), but not amplitude, reflecting a decrease in presynaptic glutamate release. In contrast, sEPSC IEI was nonsignificantly attenuated ($P = 0.0570$) following washout of U69,593 (Supplementary Fig. 3i–k), whereas sEPSC amplitude was significantly decreased ($P = 0.0307$) at the same time point (Supplementary Fig. 3i,l). Taken together, these data suggest that mOP- and dOP-LTD of excitatory transmission likely result from a reduction of presynaptic glutamate release, whereas kOP-LTD appears to have a less clear, multifaceted locus of expression.

Endogenous opioids produce LTD

Exogenous application of the endogenous opioid peptide met-enkephalin (Met-Enk) suppresses excitatory transmission in the striatum through both MOPrs and DOPrs[22]. Bath application of Met-Enk produced LTD of eEPSC amplitude in DLS MSNs (67.3 ± 3.8%; Fig. 2a) that was unaltered by pre-application of CTAP (76.8 ± 2.2%; Fig. 2b), but was blocked by NTI (97.8 ± 9.1%; Fig. 2b,c). NTI failed to reverse established Met-Enk–induced inhibition (74.6 ± 3.6%; Fig. 2c). Leu-enkephalin (Leu-Enk) induced LTD (77.1 ± 3.9%; Fig. 2d) that was modestly attenuated by pre-application of either CTAP (83.8 ± 5.2; Fig. 2e) or NTI (88.3 ± 3.5%). The nonselective opioid receptor antagonist naloxone completely blocked (96.5 ± 4.6%; Fig. 2e,f), but did not reverse (71.6 ± 7.4%; Fig. 2f), Leu-Enk–induced depression. Dynorphin A also produced LTD (71.0 ± 4.3%; Fig. 2g) that was not significantly altered ($P > 0.05$) by CTAP (88.0 ± 5.4%; Fig. 2h), but completely blocked by nor-BNI (100.8 ± 5.1%; Fig. 2h,i). Once established, dynorphin-induced LTD was not reversed by nor-BNI (75.6 ± 4.2%; Fig. 2i).

To determine whether endogenously released opioid peptides could induce LTD similar to exogenously applied ligands, we bath applied peptidase inhibitors to increase synaptic content of endogenous opioids. The neprilysin inhibitor bestatin reduced eEPSC amplitude (82.1 ± 2.2%; Fig. 3a) to a lesser extent than Met-Enk, Leu-Enk and dynorphin, as did DL-thiorphan and captopril, which are inhibitors of aminopeptidase N and angiotensin converting enzyme, respectively (DL-thiorphan, 90.2 ± 3.6%; captopril, 90.9 ± 4.0%; Fig. 3a). A cocktail of the three peptidase inhibitors robustly reduced eEPSC amplitude (64 ± 7.0%; Fig. 3a,b). Naloxone completely blocked (100.5 ± 4.1%; Fig. 3c,d), but did not reverse (74.8 ± 5.0%; Fig. 3d), inhibition by the cocktail, indicating that endogenously released opioid peptides can induce OP-LTD. Pre-application of selective antagonists for MOPrs, DOPrs and KOPrs each blocked the effects of the peptidase inhibitor cocktail (Fig. 3c). These data implicate each opioid receptor in mediating the OP-LTD induced by the

peptidase inhibitor treatment and indicate that a mixed population of endogenous opioids is released from cells in the striatum.

Consistent with a presynaptic locus of OP-LTD expression, peptidase inhibitor treatment induced a prolonged increase in PPR (1.10 ± 0.04 to 1.24 ± 0.04; Fig. 3e). When coupled with electrical stimulation (0.05 Hz, as in eEPSC experiments) during the 5-min application window, peptidase inhibitor treatment produced a prolonged increase in sEPSC IEI (Fig. 4a,b) that was blocked by pre-application of naloxone (Fig. 4b). In the absence of electrical stimulation, the peptidase inhibitor cocktail had no effect on sEPSC IEI (Fig. 4b), suggesting that the inhibitors alone failed to promote sufficient endogenous opioid signaling to induce OP-LTD. sEPSC amplitude did not change in any of these experiments (data not shown). Together, these data reveal that endogenous opioids act on opioid receptors to suppress presynaptic glutamate release in the DLS.

Given that electrical stimulation was necessary to produce endogenous OP-LTD (Fig. 4b), we probed the mechanisms underlying activity- dependent opioid peptide release. We found no role of dopamine signaling in OP-LTD, as combined application of the dopamine D1 and D2 receptor antagonists sulpiride and SCH23390 did not affect LTD induced following peptidase inhibition (75.8 ± 5.3%; Fig. 4c). In light of recent evidence of LTD in hypothalamic parvocellular neuroendocrine cells mediated by postsynaptic calcium- and mGluR-dependent opioid peptide release[15,17], we assessed the contribution of these signaling pathways in OP-LTD. Inclusion of either the calcium chelator BAPTA (65.3 ± 4.7%) or the GDP analog GDPβS (81.5 ± 4.4%) in the intrapipette solution failed to alter peptidase inhibitor–mediated LTD (Fig. 4c). However, combined bath application of the mGluR1 and mGluR5 antagonists JNJ16259685 and MPEP (91.4 ± 4.1%), as well as application of MPEP alone (96.5 ± 6.2%), but not JNJ16259685 alone (75.6 ± 2.8%), completely blocked peptidase inhibitor–induced OP-LTD (Fig. 4c,d). These results indicate a critical role for mGluR5 signaling in the activity-dependent release of opioid peptides underlying striatal OP-LTD and suggest that opioid peptides originating from the recorded MSN are not necessary to produce LTD.

mOP- and dOP-LTD operate independently

Given that mOP- and dOP-LTD are both expressed presynaptically and in MSNs throughout the dorsal striatum, we assessed whether mOP- and dOP-LTD are in fact dissociable forms of plasticity. To do so, we applied DAMGO and DPDPE sequentially. Following induction of stable mOP-LTD by DAMGO (71.6 ± 4.2%; Fig. 5a), DPDPE further decreased eEPSC amplitude (60.5 ± 4.2% of original baseline). Conversely, following stable dOP-LTD induction by DPDPE (85.1 ± 1.2%; Fig. 5b), DAMGO induced further depression of eEPSC amplitude (73.7 ± 4.4% of original baseline). These data suggest that MOPr and DOPr activation induce dissociable forms of LTD in the dorsal striatum.

Endocannabinoid-mediated LTD, induced by pairing postsynaptic MSN depolarization with trains of high-frequency presynaptic stimulation, is a prominent form of plasticity in the DLS[26]. We tested whether eCB-LTD interacts with mOP- and dOP-LTD in a manner that may inform the mechanisms distinguishing these two forms of OP-LTD. Following eCB-LTD induction (82.3 ± 4.0%; Fig. 5c), DAMGO induced a small reduction in eEPSC

amplitude that returned to pre-DAMGO levels (77.4 ± 5.2% of original baseline). Similarly, after DAMGO-induced mOP-LTD (76.2 ± 5.1%; Fig. 5d), eCB-LTD could not be induced (74 ± 3.9% of original baseline). These data reveal that mOP- and eCB-LTD are mutually occlusive. In contrast, following eCB-LTD induction (78.5 ± 2.9%; Fig. 5e), DPDPE produced a further depression (61.9 ± 4.5% of original baseline), and after DPDPE-induced dOP-LTD (69.9 ± 5.3%; Fig. 5f), eCB-LTD induction caused additional depression (49.4 ± 4.2% of original baseline). To determine whether the mutual occlusion of mOP- and eCB-LTD occurred at the presynaptic (receptor signaling) or postsynaptic (eCB production) level, we tested the effects of DAMGO on the depression induced by the presynaptic CB_1 receptor agonist WIN55,212-2. We found no difference between the effects of combined application of WIN55,212-2 and DAMGO and application of WIN55,212-2 alone (Supplementary Fig. 4), suggesting presynaptic occlusion between MOPr- and CB_1-mediated plasticity. Furthermore, the occlusion between mOP- and eCB-LTD was not simply a result of the recruitment of eCB signaling at CB_1 receptors by opioid receptor activation, as mOP-LTD (and dOP-LTD) occurred in the presence of the CB_1 receptor antagonist AM251 (Supplementary Fig. 5a,b). Conversely, eCB-LTD persisted in the presence of naloxone (Supplementary Fig. 5c). Taken together, these data indicate that mOP-LTD, but not dOP-LTD, is mutually occlusive with eCB-LTD at the presynaptic signaling level, further supporting the hypothesis that MOPrs and DOPrs exert similar, but dissociable, effects on excitatory transmission in the dorsal striatum.

One possible explanation for the dissociable nature of mOP- and dOP-LTD suggested by the pharmacological experiments is that the two receptors are expressed at synapses arising from different striatal inputs. Given that electrical stimulation at the border of the DLS and overlying white matter can nonselectively recruit both corticostriatal and thalamostriatal projections to the striatum, we virally expressed adeno-associated viral (AAV) vectors encoding a channelrhodopsin-2 (ChR2)-Venus fusion protein in the motor cortex or thalamic nuclei (targeting the central lateral and medial thalamic nuclei primarily) to test this hypothesis. Both cortical and thalamic injections of ChR2-venus resulted in robust expression in inputs to the DLS (Fig. 6a,b). DAMGO application had no clear effect on optically evoked motor cortex to striatal EPSCs (oEPSCs, 92.8 ± 2.0%; Fig. 6c), whereas it strongly inhibited thalamostriatal oEPSCs (Fig. 6c). Thalamostriatal depression appeared to slowly reverse, so these cells were recorded for up to 60 min, over which time the gradual return to baseline continued. Notably, at an end-point equivalent to the corticostriatal experiments (45 min), thalamostriatal transmission was still depressed (64.6 ± 7.3%). In contrast with DAMGO, DPDPE produced OP-LTD of corticostriatal oEPSCs (71.9 ± 3.0%; Fig. 6d), but produced little to no depression of thalamostriatal oEPSCs (90.2 ± 4.4%). Thus, MOPr and DOPr activation inhibits distinct striatal inputs, and the inhibition of thalamic inputs by MOPr activation markedly differs from that observed using electrical stimulation.

mOP- and eCB-LTD are lost after *in vivo* oxycodone exposure

The commonly prescribed and abused analgesic oxycodone is primarily a MOPr agonist[28,29]. We tested whether *in vivo* administration of oxycodone could interfere with LTD in the dorsal striatum. Mice injected with saline (intraperitoneal) 1 h before being killed showed normal LTD in the DLS following bath application of DAMGO (75.4 ± 3.7%;

Fig. 7a), DPDPE (82.7 ± 2.6%; Fig. 7b) and U69,593 (69.3 ± 2.5%; Fig. 7c). However, in mice injected with oxycodone (1 mg per kg of body weight, intraperitoneal) 1 h before death, DAMGO-induced mOP-LTD was abolished (92.2 ± 5.3%; Fig. 7a), whereas DPDPE-induced dOP-LTD remained intact (77.7 ± 4.8%; Fig. 7b). U69,593-induced kOP-LTD was preserved, but was significantly diminished (81.9 ± 1.1%, $P = 0.0195$; Fig. 7c). Peptidase inhibitor-induced LTD was also abolished in oxycodone-treated mice (saline, 81.5 ± 2.3%; oxycodone, 100.0 ± 1.4%; Fig. 7d). Consistent with evidence that mOP-LTD and eCB-LTD are mutually occlusive, eCB-LTD was absent in mice injected with oxycodone (saline, 77.6 ± 5.6%; oxycodone, 95.6 ± 6.6%; Fig. 7e). The disruption of eCB-LTD appeared to occur at, or downstream of, the level of CB_1 receptor activation, as LTD caused by bath application of the CB_1 receptor agonist WIN 55-212-2 was reduced in oxycodone-treated mice (saline, 72.8.5 ± 3.6%; oxycodone, 88.5 ± 2.7%; Fig. 7f).

To probe the persistence of the effects of oxycodone on plasticity, we killed mice up to 4 d after an injection of oxycodone or saline and tested them for mOP-LTD induction. DAMGO failed to induce mOP-LTD in oxycodone-injected mice, relative to saline-injected mice, for up to 2 d post-injection, with full recovery at 4 d (Fig. 7g,h). Taken together, these data are consistent with the notion that *in vivo* oxycodone exposure causes long-lasting disruptions in the subsequent induction of mOP- and eCB-LTD, but not dOP- or kOP-LTD.

DISCUSSION

We observed several distinct forms of OP-LTD mediated by MOPrs, DOPrs and KOPrs at excitatory synapses in the dorsal striatum. mOP- and dOP-LTD were both expressed presynaptically and throughout the dorsal striatum, but were dissociable in that they summated, differentially occluded eCB-LTD and likely inhibited different striatal inputs. In contrast, kOP-LTD was less clearly presynaptic and occurred in the DLS, but not the DMS. Application of peptidase inhibitors revealed that endogenously released opioid peptides acting through MOPrs, DOPrs and KOPrs can induce robust OP-LTD. Furthermore, acute *in vivo* exposure to the opiate analgesic oxycodone selectively interfered with mOP-LTD and eCB-LTD for up to 2 d following drug exposure. Although these data are the first, to the best of our knowledge, to show OP-LTD in striatum, OP-LTD has been described at excitatory synapses in hypothalamus[14] and inhibitory synapses in hypothalamus[17] and hippocampus[16], mediated by KOPrs, MOPrs and DOPrs, respectively. Opioids have also been shown to modulate the induction or expression of both LTD and long-term potentiation[12,13,30–32]. In addition, transient or reversible suppression of excitatory transmission by opioid receptor signaling has been reported in other brain areas, including the nucleus accumbens[33].

Our findings help inform previous reports on opioid receptor function in the dorsal striatum. Evidence that antidromic activation of pallidal-projecting MSNs produces a MOPr-mediated inhibition of excitatory transmission in the dorsal striatum[24] suggests that enkephalins serve as the principal ligands for dorsal striatal MOPrs, as enkephalins[6], but not beta-endorphin[7], are abundantly expressed in the dorsal striatum. Consistent with this view, we found that Leu-Enk induced OP-LTD that was partially blocked by the MOPr antagonist CTAP. Considered alongside evidence that consumption of highly palatable food causes a surge of

enkephalin in the DMS and that infusion of DAMGO into the DMS stimulates such consumption[34], these findings point to an important role for enkephalin action at MOPrs in striatal function. Of course, enkephalins also act on DOPrs[22], and behaviors such as ethanol consumption are known to be regulated by DOPrs in the dorsal striatum[35]. Furthermore, our findings identify a role for KOPrs in the dorsal striatum, whereas no clear KOPr- mediated synaptic effects have previously been observed. In fact, the lack of kOP-LTD in the DMS reported here may explain why a previous study[22] failed to find KOPr-mediated plasticity in the dorsal striatum, if recordings were not made exclusively in the DLS.

Using peptidase inhibitors, we found a form of striatal LTD mediated by endogenously released opioid peptides. Consistent with the known redundancy in the proteolytic actions of peptidases against striatal Met-Enk[36] and opioid peptides more generally, endogenous OP-LTD was greatest when three peptidase inhibitors were used in combination. The fact that MOPr, DOPr and KOPr antagonists each partially reversed the LTD induced by the peptidase inhibitor cocktail suggests enhanced levels of both enkephalin and dynorphin. Our data also argue against a basal opioid peptide tone in the dorsal striatum, as the peptidase inhibitors failed to modify sEPSC frequency in the absence of electrical stimulation. This electrical stimulation appeared to provide the requisite glutamate to activate mGluR5 receptors and thereby promote opioid peptide release, similar to the mechanism of opioid release observed in the hypothalamus[17]. Unlike in the hypothalamus, however, the opioid peptides critical for the expression of striatal OP-LTD did not appear to originate from the recorded cell. Furthermore, numerous attempts to drive broader MSN activity independent of electrical afferent stimulation failed to produce peptidase inhibitor OP-LTD (data not shown), suggesting that GABAergic afferent and postsynaptic activation is insufficient for striatal OP-LTD, at least in our preparation. mGluR5-mediated opioid peptide release therefore appears to be a heterosynaptic phenomenon involving the diffusion of opioid peptides from their release sites to the synapses being probed.

The ability of MOPr and DOPr activation to induce dissociable forms of OP-LTD, as evidenced by their additive effects and differential occlusion with eCB-LTD and *in vivo* oxycodone exposure, is likely to arise from two possible scenarios. First, MOPrs and DOPrs may inhibit excitatory transmission through different downstream mechanisms. However, MOPrs and DOPrs are both $G_{i/o}$-coupled GPCRs, and likely couple to similar effectors. A more likely alternative is that MOPrs and DOPrs inhibit transmission at different excitatory terminals in striatum. Electron microscopy of rat striatum revealed that MOPrs and DOPrs are rarely coexpressed on the same terminals, and instances of coexpression tend to occur on inhibitory, rather than excitatory, terminals[37]. Furthermore, *in situ* hybridization studies of rat brain found that MOPr mRNA is more densely expressed than DOPr mRNA in the thalamus; the opposite has been observed in many cortical areas known to project to the dorsal striatum[38,39]. Consistent with these studies, we found that DOPr activation had little effect on thalamostriatal transmission, but induced LTD of inputs from motor cortex. In contrast, we found that MOPr activation produced no clear effect on these motor cortical inputs, but robustly depressed thalamostriatal transmission. Notably, this latter MOPr-mediated suppression does not model our electrical stimulation data well, nor does it appear to necessarily be LTD.

Two possible scenarios may account for the differences between electrically and optogenetically identified MOPr-mediated plasticity. First, MOPr-mediated depression may selectively occur at thalamostriatal inputs, and the mixed population of inputs activated by electrical stimulation, including a subset of the thalamostriatal inputs recruited by optogenetic activation, may exhibit a kinetically different form of MOPr-mediated depression. We could speculate that electrical stimulation preferentially activates cortical inputs, given our placement of the stimulating electrode at the border of the dorsal striatum and overlying white matter and the predominant innervation of MSNs by cortical versus thalamic inputs[40]. Alternatively, electrical stimulation may activate unidentified, presumably non-motor cortical, inputs that display mOP-LTD independent of the MOPr-mediated depression observed at thalamostriatal inputs. MOPr mRNA has been detected in other non-motor cortical regions[38,39]; thus, striatal inputs from these areas may be important sites of mOP-LTD expression.

Our data reveal a selective interaction between CB_1 and MOPr signaling, but not DOPr or KOPr signaling, in the dorsal striatum. These findings extend prior reports of a cannabinoid-MOPr interaction[41]. For example, rats chronically treated with CB_1 receptor agonists show impaired eCB-LTD and MOPr-mediated suppression of excitatory transmission in the nucleus accumbens[42]. The nature of the CB_1-MOPr interaction that we observed is currently unclear, but possibly results from shared signaling pathways of CB_1 and MOPrs, as well as potential coexpression of the two receptors on the same excitatory terminals in the dorsal striatum. Notably, our data indicate that eCB- and mOP-LTD are not mutually dependent, as inhibiting one did not impair induction of the other. The basis of the dissociation between eCB- and dOP-LTD is similarly unknown, but is consistent with our evidence that mOP- and dOP-LTD are distinct. CB_1 receptors display a graded mediolateral expression profile in striatum, with the highest expression laterally[43], whereas MOPrs and DOPrs are more uniform in their expression[44]. Given that these DMS and DLS subregions are preferentially recruited during different aspects of action learning and selection[18], opioid- and eCB-mediated forms of plasticity in the striatum are likely to have unique roles in striatal-dependent behavior.

A single, non-contingent exposure to oxycodone induced long-lasting disruptions in MOPr- and CB_1 receptor–mediated striatal plasticity, leaving dOP- and kOP-LTD intact. Given that oxycodone and its principal metabolite oxymorphone more selectively bind to MOPrs than other opioid receptors[28,29], it is plausible that oxycodone treatment induces a form of mOP-LTD in the dorsal striatum that occludes subsequent *ex vivo* attempts to induce MOPr- and CB_1-LTD. This is an attractive possibility given that induction of mOP-LTD occludes CB_1-LTD expression. An alternative explanation for oxycodone's effect is that oxycodone treatment may lead to long-lasting MOPr desensitization. Arguing against this explanation, however, presynaptic opioid receptors, such as those thought to contribute to striatal OP-LTD, are more resistant to desensitization than their post-synaptic counterparts[45,46]. Opioid receptor downregulation or alterations in receptor-effector coupling may also be involved in the effects of oxycodone on mOP-LTD. The behavioral effects of oxycodone-induced changes in striatal plasticity are also currently unknown. Recent reports have shown that chronic exposure to alcohol[47] or Δ9-tetrahydrocannabinol[48] that disrupt dorsal striatal eCB-

LTD also modify dorsal striatal–dependent learning, including the transition from goal-directed to habitual responding[48]. These findings suggest that similar behavioral adaptations could occur following oxycodone exposure, and potentially contribute to the transition from controlled to compulsive opioid use.

In summary, we observed previously unknown opioid-mediated forms of long-term striatal plasticity that are differentially affected by opioid analgesic exposure. Exogenously applied and endogenously released opioid peptides induced robust OP-LTD of excitatory transmission in the dorsal striatum. MOPr, DOPr and KOPr activation induced distinct, yet parallel, forms of OP-LTD. The subregion specificity of kOP-LTD and input specificity of mOP- and dOP-LTD provide a foundation for new hypotheses regarding the role of opioid receptors in modulating specific components of striatal-based behaviors. As we learn more about the developmental and behavioral roles for opioid and eCB signaling in the striatum, the long-lasting disruptions to MOPr- and CB_1-mediated striatal plasticity seen following acute exposure to a commonly used and abused prescription analgesic are likely to become increasingly relevant to clinical practice.

ONLINE METHODS

Animals and materials

All animal care and experimental procedures used in this study were approved by the Institutional Animal Care and Use Committee of the National Institute on Alcohol Abuse and Alcoholism and conformed to the guidelines of the US National Institutes of Health on the Care and Use of Animals. All efforts were made to reduce the number of animals used and to minimize their suffering during procedures. Sprague-Dawley rats and C57BL/6J mice were used for brain slice electrophysiology. Animals were housed in standard 12-h light/dark cycle. Rat pups were born in house and housed with their mothers. Mice were purchased from the Jackson Laboratory and housed two per cage. Drugs and reagents were purchased from Tocris Cookson, Sigma-Aldrich or Bachem Americas.

Brain slice preparation

Brain slices were prepared according to the methods previously published[27]. Briefly, rats (males and females, P11–19 for whole-cell recordings, P20–25 for field recordings) or mice (males, P28–42) were anesthetized and brains were removed and immediately placed in 95% $C0_2$/5% O_2-bubbled, ice-cold cutting solution containing 30 mM NaCl, 4.5 mM KCl, 1 mM $MgCl_2$, 26 mM $NaHCO_3$, 1.2 mM NaH_2PO_4, 10 mM glucose and 194 mM sucrose. Coronal brain slices containing the striatum were prepared at various thicknesses (300 and 250 μm for rat and mouse whole-cell recordings, respectively; 350 μm for rat extracellular recordings) using a vibratome (Leica Microsystems, GmbH) and slices were transferred into 95% $C0_2$/5% O_2-bubbled, 32 °C artificial cerebral spinal fluid (aCSF) containing 124 mM NaCl, 4.5 mM KCl, 2 mM $CaCl_2$, 1 mM $MgCl_2$, 26 mM $NaHCO_3$, 1.2 mM NaH_2PO_4 and 10 mM glucose. Slices were incubated for 1 h at 32 °C and then moved to 24 °C.

Electrophysiology recordings

Whole-cell, voltage-clamp recordings of EPSCs from MSNs were carried out at 29–32 °C using a Multiclamp 700A amplifier (Axon Instruments). Slices were placed onto an elevated platform of nylon mesh in the recording chamber and aCSF was constantly perfused across the slice surfaces at a rate of 1 ml min^{-1}. Drugs were prepared as stock solutions and diluted in aCSF to their final concentrations and used on the same day. Drugs were administered to brain slices via bath application, in which normal aCSF was replaced with aCSF containing drug. Antagonists were present in aCSF throughout recordings in which they were used to block agonist effects. Recording pipettes of 2.4–4.0 MΩ were filled with solution containing a $CsMeSO_3$-based solution of 295–310 mOsm containing 120 mM $CsMeSO_3$, 5 mM NaCl, 10 mM TEA-Cl, 10 mM HEPES, 5 mM lidocaine bromide, 1.1 mM EGTA, 0.3 mM Na-GTP and 4 mM Mg-ATP. Picrotoxin (50 μM) was added to the aCSF for recordings to isolate excitatory transmission. Slices were visualized on an Olympus BX50W microscope (Olympus Corporation of America) using a 5×/0.10 objective for stimulating electrode placement and a 40×/0.80 water-immersion objective for localizing cells for whole-cell recordings. MSNs were identified based on their capacitance and membrane resistance. Cells were held at −60 mV throughout the course of the experiments unless otherwise indicated. For DLS recordings, a bipolar stimulating electrode was placed at the border of the white matter of the external capsule. For DMS recordings, the stimulating electrode was placed at the border of the overlying corpus callosum and DMS and recordings were performed from MSNs just lateral to the dorsolateral-most point of the lateral ventricle. eEPSCs were elicited every 20 s and intensity was adjusted to produce eEPSCs of 200–400 pA in amplitude. Endocannabinoid-LTD was induced by depolarizing the postsy-naptic MSN to 0 mV, combined with high-frequency stimulation (1 s of 100-Hz stimulation repeated every 10 s four times). To determine the synaptic site of plasticity expression, PPR analysis and sEPSC recordings were performed. Paired stimulations separated by 50 ms were delivered and the average amplitude of the second pulses (using tail current as baseline) in 5-min windows was divided by the average amplitude of the first pulses (using pre-stimulation current as baseline) in the corresponding 5-min windows to provide PPRs. PPRs greater than 1.0 were interpreted as paired-pulse facilitation. Ratios were calculated for each neuron under basal and drug-treated conditions. All whole-cell recordings were filtered at 2 kHz and digitized at 10 kHz. Data were acquired using Clampex 10.3 (Molecular Devices). Series resistance was monitored and only cells with a stable series resistance (less than 25 MΩ and that did not change more than 15%) were included for data analysis.

Extracellular field recordings were acquired from brain slices perfused with aCSF at a rate of 1.5 ml min^{-1} in a submersion chamber using glass recording electrodes filled with 0.9% NaCl solution (wt/vol). Population spikes ranging in amplitude from 0.4 to 1.5 mV were elicited every 30 s in the DLS using a twisted tungsten bipolar stimulating electrode placed just ventral to the overlaying white matter of the external capsule. Recordings were filtered at 1 kHz and digitized at 20 kHz using Clampex 8.2.

Drug exposure

Mice (males, P28–42) were injected intraperitoneal with 1 mg per kg oxycodone dissolved in 0.9% NaCl saline (Hospira) or an equivalent volume of saline vehicle. Each mouse from a pair of cage mates was randomly selected for saline or oxycodone treatment. Between 1 h and 4 d after injection, mice were killed and brain slices were obtained for electrophysiological recordings (as described above). Recordings were made 2–7 h after death.

Viral injections and optogenetic experiments

Male C57BL/6J mice were anesthetized with isoflurane and stereotaxically injected with the adeno-associated viral (AAV) vector, AAV9.CAG.ChR2-Venus.W.SV40 (Upenn Vector Core) to drive ChR2 expression in striatal inputs. Injection coordinates are relative to bregma for A/P and M/L and brain surface for D/V. In one cohort of mice, injections (200 nl, 25 nl min^{-1} infusion rate) were made bilaterally into thalamic nuclei that project to striatum (primarily parafasicular nucleus; injection coordinates: A/P: −1.6, M/L: ±0.35, D/V: −3.4). A second cohort received two bilateral sets of injections (100 nl each, 25 nl min^{-1} infusion rate) made into M1/M2 motor cortices (coordinates: A/P: +2.2, M/L: ±1.2, D/V: −0.9 and A/P: +1.4, M/L: ±1.2, D/V: −0.75). Mice were allowed to recover for at least 3 weeks before brain slices were made. oEPSCs in MSNs were evoked in brain slices using 470-nm blue light (5-ms exposure time) delivered via field illumination using a High-Power LED Source (LED4D067, Thor Labs). Light intensity was adjusted to produce oEPSCs of 200–400-pA magnitude (<100 mW). oEPSCs were evoked once per minute. Imaging of brain slices was performed using an Olympus MVX10 microscope (Olympus Corporation of America).

Statistical analysis

Measurements of EPSCs and population spikes were made using pClamp software (Molecular Devices). All graphs and statistical analyses were generated using GraphPad Prism 4.0 software (Hearne Scientific Software) or MiniAnalysis (Synaptosoft). Data are reported as mean ± s.e.m. eEPSC and population spike data were averaged per min for all recordings, except for PPR analysis, which used EPSCs averaged per 5 min. eEPSC and population spike data are reported as percent of baseline. Percent baseline measurements of eEPSCs, oEPSCs and population spikes reported in the text for time courses presented in the figures are the average of the final 10 min of recordings. Percent baseline values reported in the text for summary plot figures are the average of the 10-min time window beginning 10 min after drug application was terminated. Statistical analyses were performed on these same time windows. For PPR data, the first and last 5-min bin data are reported in the text. For sEPSC recordings, data are reported for 5-min time windows for basal, post-drug application and wash conditions. Data from Figure 5 are reported in the text as the final 5 min before the second drug/stimulus application and the final 5 min of recording. *N* values for data from Figures 1–6 represent numbers of recorded cells; only one cell was used from each slice, and at least two, but most often more or more, animals were used for each experimental group. *N* values for data from Figure 7 represent numbers of mice used; at least five mice were used for each experimental group. No statistical methods were used to

pre-determine sample sizes, but our sample sizes are similar to those reported in previous publications[26,27]. Data collection and analysis were not performed blind to the conditions of the experiments. Data distribution was assumed to be normal for all eEPSC and oEPSC data, but not for sEPSC data, but this was not formally tested. Comparisons of control versus drug and antagonist block versus antagonist chase were conducted using unpaired two-tailed Student's *t* tests. Paired Student's *t* tests were used to compare saline versus oxycodone. Comparisons of agonists versus various antagonists, PPRs and individual peptidase inhibitors versus the cocktail were conducted using one-way ANOVA with Dunnett's post-test. sEPSC data were analyzed using the Friedman test with Dunn's post-test. Cumulative probability curves were not evaluated statistically, but presented only for qualitative assessment. Two-way repeated-measures ANOVA with Sidak's post-test were used to assess the effects of oxycodone across days after exposure. Alpha was set at 0.05. Statistical significance is indicated as $*P < 0.05$, $**P < 0.01$ and $***P < 0.0001$.

Supplementary Material

Refer to Web version on PubMed Central for supplementary material.

Acknowledgments

We extend special thanks to W. Xiong for his efforts in performing preliminary experiments for this study. This research was supported by the Division of Intramural Clinical and Biological Research of the National Institute on Alcohol Abuse and Alcoholism, US National Institutes of Health.

References

1. Cicero TJ, Inciardi JA, Muñoz A. Trends in abuse of oxycontin and other opioid analgesics in the United States: 2002–2004. J Pain. 2005; 6:662–672. [PubMed: 16202959]
2. Compton WM, Volkow ND. Major increases in opioid analgesic abuse in the United States: concerns and strategies. Drug Alcohol Depend. 2006; 81:103–107. [PubMed: 16023304]
3. Manubay JM, Muchow C, Sullivan MA. Prescription drug abuse: epidemiology, regulatory issues, chronic pain management with narcotic analgesics. Prim Care. 2011; 38:71–90. [PubMed: 21356422]
4. Ordóñez Gallego A, González Barón M, Espinosa Arranz E. Oxycodone: a pharmacological and clinical review. Clin Transl Oncol. 2007; 9:298–307. [PubMed: 17525040]
5. Le Merrer J, Becker JAJ, Befort K, Kieffer BL. Reward processing by the opioid system in the brain. Physiol Rev. 2009; 89:1379–1412. [PubMed: 19789384]
6. Fallon JH, Leslie FM. Distribution of dynorphin and enkephalin peptides in the rat brain. J Comp Neurol. 1986; 249:293–336. [PubMed: 2874159]
7. Finley JC, Lindström P, Petrusz P. Immunocytochemical localization of beta-endorphin–containing neurons in the rat brain. Neuroendocrinology. 1981; 33:28–42. [PubMed: 6265819]
8. Noble F, et al. First discrete autoradiographic distribution of aminopeptidase N in various structures of rat brain and spinal cord using the selective iodinated inhibitor [^{125}I]RB 129. Neuroscience. 2001; 105:479–488. [PubMed: 11672613]
9. Strittmatter SM, Lo MM, Javitch JA, Snyder SH. Autoradiographic visualization of angiotensin-converting enzyme in rat brain with [^{3}H]captopril: localization to a striatonigral pathway. Proc Natl Acad Sci USA. 1984; 81:1599–1603. [PubMed: 6324207]
10. Waksman G, Hamell E, Delay-Goyet P, Roques BP. Neuronal localization of the neutral endopeptidase 'enkephalinase' in rat brain revealed by lesions and autoradiography. EMBO J. 1986; 5:3163–3166. [PubMed: 3545813]

11. Dacher M, Nugent FS. Opiates and plasticity. Neuropharmacology. 2011; 61:1088–1096. [PubMed: 21272593]
12. Dacher M, Nugent FS. Morphine-induced modulation of LTD at GABAergic synapses in the ventral tegmental area. Neuropharmacology. 2011; 61:1166–1171. [PubMed: 21129388]
13. Drake CT, Chavkin C, Milner TA. Opioid systems in the dentate gyrus. Prog Brain Res. 2007; 163:245–263. [PubMed: 17765723]
14. Iremonger KJ, Bains JS. Retrograde opioid signaling regulates glutamatergic transmission in the hypothalamus. J Neurosci. 2009; 29:7349–7358. [PubMed: 19494156]
15. Iremonger KJ, Kuzmiski JB, Baimoukhametova DV, Bains JS. Dual regulation of anterograde and retrograde transmission by endocannabinoids. J Neurosci. 2011; 31:12011–12020. [PubMed: 21849561]
16. Piskorowski RA, Chevaleyre V. Delta-opioid receptors mediate unique plasticity onto parvalbumin-expressing interneurons in area CA2 of the hippocampus. J Neurosci. 2013; 33:14567–14578. [PubMed: 24005307]
17. Wamsteeker Cusulin JI, Füzesi T, Inoue W, Bains JS. Glucocorticoid feedback uncovers retrograde opioid signaling at hypothalamic synapses. Nat Neurosci. 2013; 16:596–604. [PubMed: 23563581]
18. Lovinger DM. Neurotransmitter roles in synaptic modulation, plasticity and learning in the dorsal striatum. Neuropharmacology. 2010; 58:951–961. [PubMed: 20096294]
19. Smith Y, Raju DV, Pare J, Sidibe M. The thalamostriatal system: a highly specific network of the basal ganglia circuitry. Trends Neurosci. 2004; 27:520–527. [PubMed: 15331233]
20. Voorn P, Vanderschuren LJMJ, Groenewegen HJ, Robbins TW, Pennartz CMA. Putting a spin on the dorsal-ventral divide of the striatum. Trends Neurosci. 2004; 27:468–474. [PubMed: 15271494]
21. Tepper JM, Abercrombie ED, Bolam JP. Basal ganglia macrocircuits. Prog Brain Res. 2007; 160:3–7. [PubMed: 17499105]
22. Jiang ZG, North RA. Pre- and postsynaptic inhibition by opioids in rat striatum. J Neurosci. 1992; 12:356–361. [PubMed: 1309576]
23. Miura M, Saino-Saito S, Masuda M, Kobayashi K, Aosaki T. Compartment-specific modulation of GABAergic synaptic transmission by μ-opioid receptor in the mouse striatum with green fluorescent protein–expressing dopamine islands. J Neurosci. 2007; 27:9721–9728. [PubMed: 17804632]
24. Blomeley CP, Bracci E. Opioidergic interactions between striatal projection neurons. J Neurosci. 2011; 31:13346–13356. [PubMed: 21940429]
25. Wilson CJ, Kawaguchi Y. The origins of two-state spontaneous membrane potential fluctuations of neostriatal spiny neurons. J Neurosci. 1996; 16:2397–2410. [PubMed: 8601819]
26. Gerdeman GL, Ronesi J, Lovinger DM. Postsynaptic endocannabinoid release is critical to long-term depression in the striatum. Nat Neurosci. 2002; 5:446–451. [PubMed: 11976704]
27. Mathur BN, Capik NA, Alvarez VA, Lovinger DM. Serotonin induces long-term depression at corticostriatal synapses. J Neurosci. 2011; 31:7402–7411. [PubMed: 21593324]
28. Monory K, et al. Opioid binding profiles of new hydrazone, oxime, carbazone and semicarbazone derivatives of 14-alkoxymorphinans. Life Sci. 1999; 64:2011–2020. [PubMed: 10374926]
29. Yoburn BC, Shah S, Chan K, Duttaroy A, Davis T. Supersensitivity to opioid analgesics following chronic opioid antagonist treatment: relationship to receptor selectivity. Pharmacol Biochem Behav. 1995; 51:535–539. [PubMed: 7667382]
30. Francesconi W, Berton F, Demuro A, Madamba SG, Siggins GR. Naloxone blocks long-term depression of excitatory transmission in rat CA1 hippocampus *in vitro*. Arch Ital Biol. 1997; 135:37–48. [PubMed: 9139581]
31. Wagner JJ, Etemad LR, Thompson AM. Opioid-mediated facilitation of long-term depression in rat hippocampus. J Pharmacol Exp Ther. 2001; 296:776–781. [PubMed: 11181906]
32. Drdla-Schutting R, Benrath J, Wunderbaldinger G, Sandkühler J. Erasure of a spinal memory trace of pain by a brief, high-dose opioid administration. Science. 2012; 335:235–238. [PubMed: 22246779]

33. Hoffman AF, Lupica CR. Direct actions of cannabinoids on synaptic transmission in the nucleus accumbens: a comparison with opioids. J Neurophysiol. 2001; 85:72–83. [PubMed: 11152707]
34. DiFeliceantonio AG, Mabrouk OS, Kennedy RT, Berridge KC. Enkephalin surges in dorsal neostriatum as a signal to eat. Curr Biol. 2012; 22:1918–1924. [PubMed: 23000149]
35. Nielsen CK, et al. δ-opioid receptor function in the dorsal striatum plays a role in high levels of ethanol consumption in rats. J Neurosci. 2012; 32:4540–4552. [PubMed: 22457501]
36. Hiranuma T, Oka T. Effects of peptidase inhibitors on the [Met5]-enkephalin hydrolysis in ileal and striatal preparations of guinea-pig: almost complete protection of degradation by the combination of amastatin, captopril and thiorphan. Jpn J Pharmacol. 1986; 41:437–446. [PubMed: 3534399]
37. Wang H, Pickel VM. Preferential cytoplasmic localization of δ-opioid receptors in rat striatal patches: comparison with plasmalemmal μ-opioid receptors. J Neurosci. 2001; 21:3242–3250. [PubMed: 11312309]
38. George SR, et al. Distinct distributions of mu, delta and kappa opioid receptor mRNA in rat brain. Biochem Biophys Res Commun. 1994; 205:1438–1444. [PubMed: 7802680]
39. Mansour A, et al. Mu, delta and kappa opioid receptor mRNA expression in the rat CNS: an *in situ* hybridization study. J Comp Neurol. 1994; 350:412–438. [PubMed: 7884049]
40. Huerta-Ocampo I, Mena-Segovia J, Bolam JP. Convergence of cortical and thalamic input to direct and indirect pathway medium spiny neurons in the striatum. Brain Struct Funct. Jul 6.2013 published online. 10.1007/s00429-013-0601-z
41. López-Moreno JA, López-Jiménez A, Gorriti MA, Rodríguez de Fonseca F. Functional interactions between endogenous cannabinoid and opioid systems: Focus on alcohol, genetics and drug-addicted behaviors. Curr Drug Targets. 2010; 11:406–428. [PubMed: 20196742]
42. Hoffman AF, Oz M, Caulder T, Lupica CR. Functional tolerance and blockade of long-term depression at synapses in the nucleus accumbens after chronic cannabinoid exposure. J Neurosci. 2003; 23:4815–4820. [PubMed: 12832502]
43. Hohmann AG, Herkenham M. Localization of cannabinoid CB(1) receptor mRNA in neuronal subpopulations of rat striatum: a double-label *in situ* hybridization study. Synapse. 2000; 37:71–80. [PubMed: 10842353]
44. Tempel A, Zukin RS. Neuroanatomical patterns of the mu, delta and kappa opioid receptors of rat brain as determined by quantitative *in vitro* autoradiography. Proc Natl Acad Sci USA. 1987; 84:4308–4312. [PubMed: 3035579]
45. Fyfe LW, Cleary DR, Macey TA, Morgan MM, Ingram SL. Tolerance to the antinociceptive effect of morphine in the absence of short-term presynaptic desensitization in rat periaqueductal gray neurons. J Pharmacol Exp Ther. 2010; 335:674–680. [PubMed: 20739455]
46. Pennock RL, Hentges ST. Differential expression and sensitivity of presynaptic and postsynaptic opioid receptors regulating hypothalamic proopiomelanocortin Neurons. J Neurosci. 2011; 31:281–288. [PubMed: 21209213]
47. DePoy L, et al. Chronic alcohol produces neuroadaptations to prime dorsal striatal learning. Proc Natl Acad Sci USA. 2013; 110:14783–14788. [PubMed: 23959891]
48. Nazzaro C, et al. SK channel modulation rescues striatal plasticity and control over habit in cannabinoid tolerance. Nat Neurosci. 2012; 15:284–293. [PubMed: 22231426]

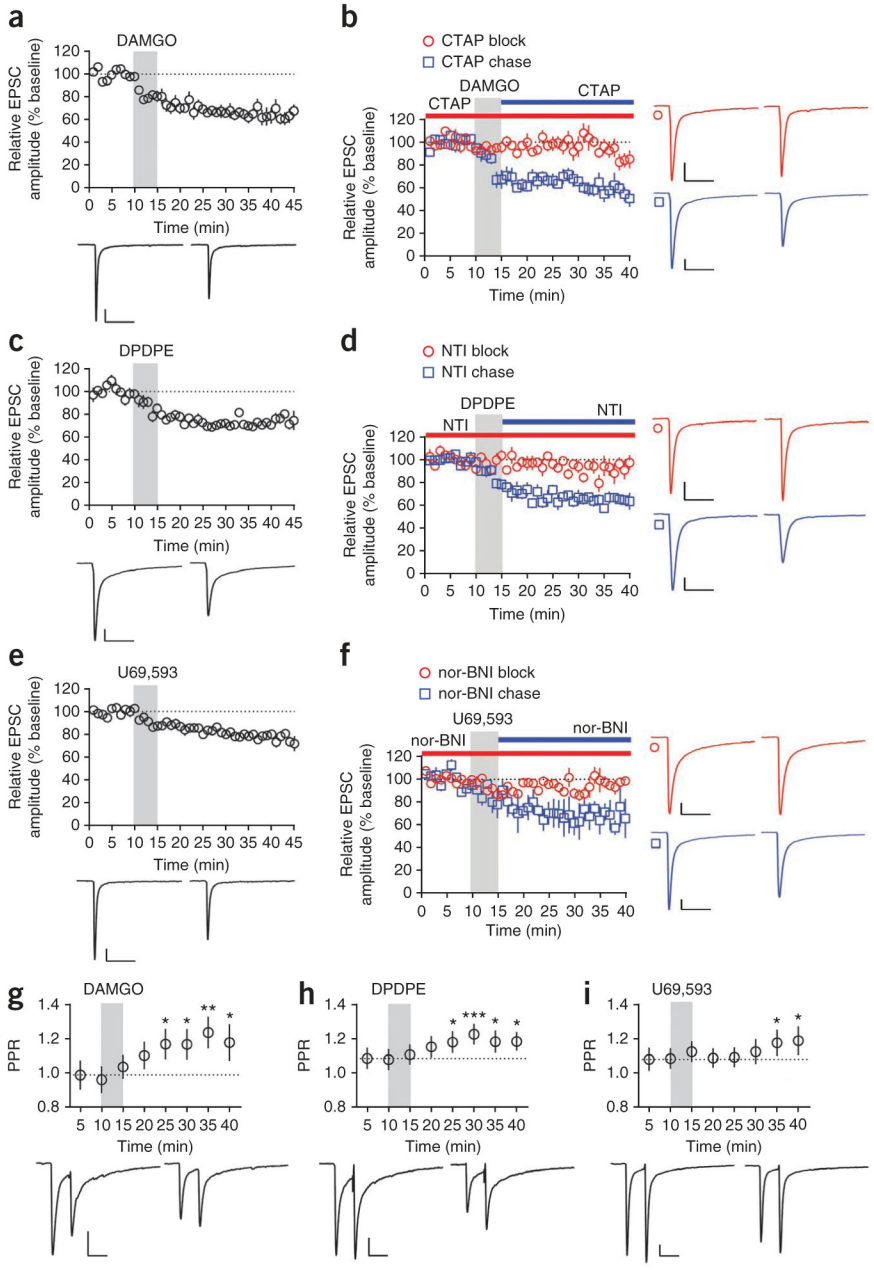

Figure 1.

Opioid receptor activation produces LTD of excitatory transmission in dorsal striatum. (**a**) DAMGO (0.3 μM, 5 min) induced mOP-LTD of eEPSC amplitude in MSNs of the rat DLS (n = 9). (**b**) The MOPr antagonist CTAP (1 μM) prevented mOP-LTD when applied before DAMGO (versus DAMGO, P = 0.0030, t_{14} = 3.590, n = 7). CTAP failed to reverse mOP-LTD when applied after DAMGO (versus CTAP block, P = 0.0011, t_{11} = 4.394, n = 6). (**c**) DPDPE (0.3 μM, 5 min) induced dOP-LTD (n = 9). (**d**) The DOPr antagonist naltrindole (NTI, 1 μM) prevented dOP-LTD (versus DPDPE, P = 0.0026, t_{12} = 3.780, n = 5). NTI failed to reverse dOP-LTD (versus NTI block, P = 0.0012, t_9 = 4.649, n = 6). (**e**) U69,593 (0.3 μM, 5 min) induced kOP-LTD (n = 10). (**f**) The KOPr antagonist nor-BNI (0.1 μM)

prevented kOP-LTD (versus U69,593, $P = 0.0066$, $t_{13} = 3.228$, $n = 5$). nor-BNI failed to reverse kOP-LTD (versus nor-BNI block, $P = 0.0499$, $t_9 = 2.264$, $n = 6$). (**g**) DAMGO (0.3 μM, 5 min) induced a long-lasting increase in the PPR of eEPSC amplitude in MSNs of the DLS ($P = 0.0002$, $F_{7,56} = 4.981$, $n = 9$). (**h**) DPDPE (0.3 μM, 5 min) produced a long-lasting increase in PPR ($P < 0.0001$, $F_{7,91} = 5.210$, $n = 14$). (**i**) U69,593 (0.3 μM, 5 min) produced a delayed increase in PPR ($P = 0.0081$, $F_{7,63} = 3.041$, $n = 10$). Representative traces are the average of the first 10 min (first of each pair) and the final 10 min (second of each pair) of recording. Scale bars represent 50 pA, 50 ms. All error bars indicate s.e.m. Data in **a**–**f** were analyzed with unpaired Student's *t*-test. Data in **g**–**i** were analyzed with a repeated-measures ANOVA with Dunnett's multiple comparisons post-test versus 5 min. *$P < 0.05$, **$P < 0.01$, ***$P < 0.001$.

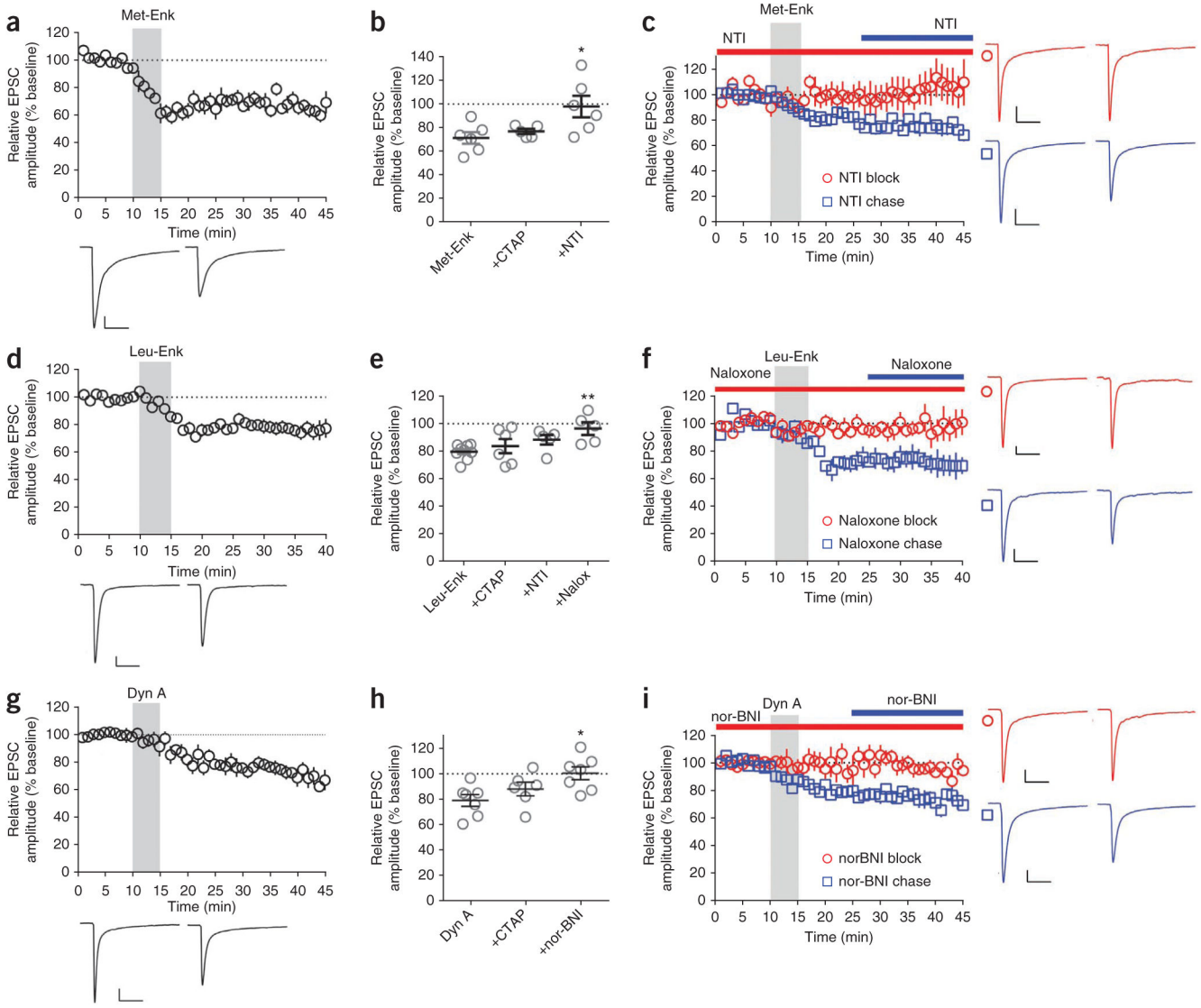

Figure 2.

Bath application of endogenous opioid peptides produces OP-LTD. (**a**) Met-Enk (10 μM, 5 min) produced LTD of eEPSC amplitude (n = 6). (**b**) Met-Enk–induced OP-LTD (n = 6) was induced in the presence of CTAP (1 μM, n = 5), but was prevented in the presence of NTI (1 μM, n = 6) (P = 0.0246, $F_{2,14}$ = 4.883). (**c**) NTI blocked (n = 6), but did not reverse, Met-Enk–induced OP-LTD (versus NTI block, P = 0.0649, t_9 = 2.102, n = 5). (**d**) Leu-Enk (10 μM, 5 min) produced OP-LTD (n = 9). (**e**) Neither CTAP (1 μM, n = 6) nor NTI (1 μM, n = 5) blocked Leu-Enk–induced OP-LTD (P = 0.0231, $F_{3,21}$ = 3.907). However, naloxone (nalox, 2 μM) completely blocked Leu-Enk–induced OP-LTD (n = 5). (**f**) Naloxone blocked (n = 5), but did not reverse, Leu-Enk–induced OP-LTD (versus naloxone block, P = 0.0407, t_9 = 2.387, n = 6). (**g**) Dynorphin A (Dyn A, 1 μM, 5 min) produced OP-LTD (n = 7). (**h**) Dyn A–induced OP-LTD was induced in the presence of CTAP (1 μM, n = 6), but was prevented in presence of nor-BNI (0.1 μM, n = 7) (P = 0.0214, $F_{2,17}$ = 4.860). (**i**) nor-BNI blocked (n = 6), but did not reverse, Dyn A–induced OP-LTD (versus nor-BNI block, P =

0.0086, $t_9 = 3.346$, $n = 5$). Representative traces are the average of the first 10 min (first of each pair) and the final 10 min (second of each pair) of recording. Scale bars represent 50 pA, 50 ms. All error bars indicate s.e.m. Data in **a**,**c**,**d**,**f**,**g**,**i** were analyzed with Student's *t* test (paired, drug versus baseline; unpaired, block versus chase). Data in **b**,**e**,**h** were analyzed with one-way ANOVA with Tukey's post-test. *$P < 0.05$, **$P < 0.01$.

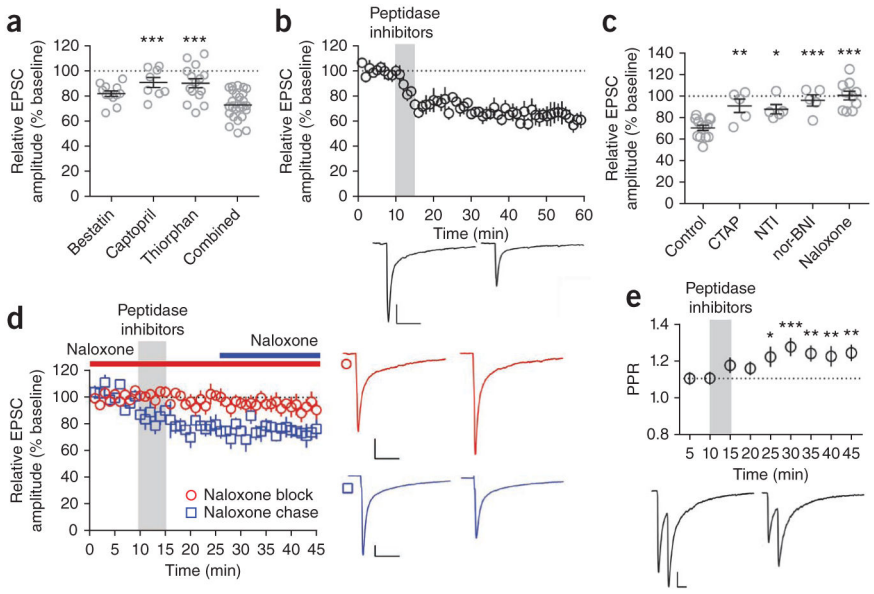

Figure 3.

Endogenously released opioid peptides induce OP-LTD. (**a**) Bath application (5 min) of the peptidase inhibitors bestatin (10 μM, $n = 12$), captopril (10 μM, $n = 8$) and DL-thiorphan (1 μM, $n = 15$), or a combination of the three, induced LTD of eEPSC magnitude ($n = 25$) ($P < 0.0001$, $F_{3,56} = 9.366$). (**b**) The peptidase inhibitors induced LTD ($n = 5$). (**c**) CTAP (1 μM, $n = 5$) and nor-BNI (100 nM, $n = 5$) blocked, and NTI (1 μM, $n = 5$) partially blocked, the LTD induced by peptidase inhibitors. Naloxone (2 μM, $n = 6$) completely blocked LTD ($P < 0.0001$, $F_{4,33} = 11.51$). (**d**) Naloxone blocked ($n = 6$), but did not reverse, the LTD induced by peptidase inhibitors (versus naloxone block, $P = 0.0305$, $t_9 = 2.565$, $n = 5$). (**e**) Peptidase inhibitors increased the PPR of eEPSC amplitude ($P < 0.0001$, $F_{8,144} = 5.714$, $n = 27$). Representative traces are the average of the first 10 min (first of each pair) and the final 10 min (second of each pair) of recording. Scale bars represent 50 pA, 50 ms. All error bars indicate s.e.m. Data in **a**,**c**,**e** were analyzed with one-way ANOVA with Dunnett's multiple comparisons post-test. Data in **b**,**d** were analyzed with unpaired Student's *t* test. $*P < 0.05$, $**P < 0.01$, $***P < 0.001$.

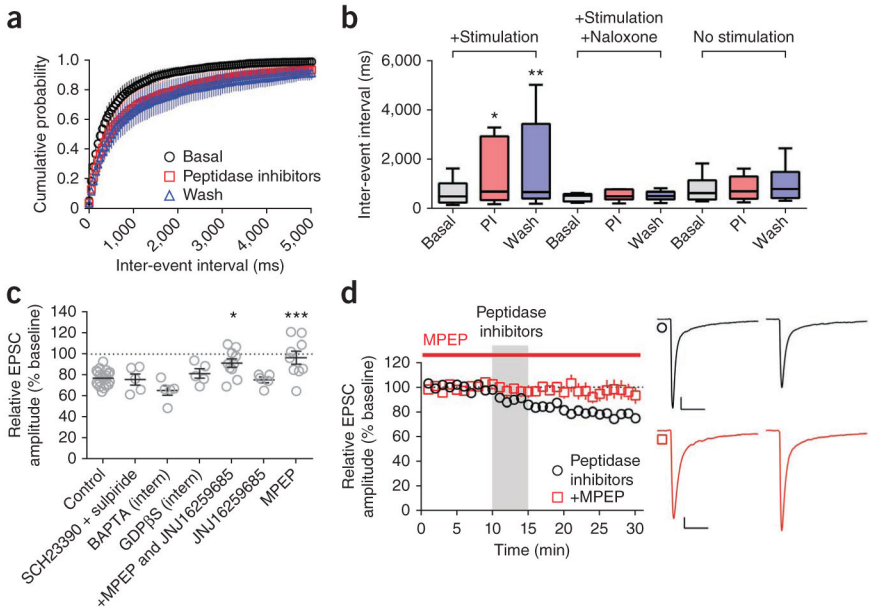

Figure 4.

Endogenous opioids are released in an mGluR5 and activity-dependent manner. (**a**,**b**) Electrical stimulation (0.05 Hz) during the application of peptidase inhibitors increased the sEPSC IEI ($P = 0.0008$, Friedman statistic = 12.60, $n = 10$). (**b**) Naloxone blocked the effect of the inhibitors paired with stimulation ($P = 0.7402$, Friedman statistic = 1.000, $n = 6$). Without electrical stimulation, the peptidase inhibitors (PI) did not alter sEPSC IEI ($P = 0.2192$, Friedman statistic = 3.455, $n = 11$). (**c**) Peptidase inhibitors induced OP-LTD in the presence of the dopamine receptor antagonists SCH23390 and sulpiride (2 μM each, $n = 5$), intrapipette membrane-impermeable BAPTA (20 mM, $n = 5$), or intrapipette GDPβS (2 mM, $n = 5$). Combined application of the mGluR1 antagonist (JNJ16259685, 0.75 μM) and the mGluR5 antagonist MPEP (10 μM), prevented OP-LTD induced by the peptidase inhibitors ($n = 10$). JNJ16259685 alone failed to inhibit the peptidase inhibitor–induced LTD ($n = 5$). MPEP alone prevented peptidase inhibitor–induced OP-LTD ($n = 9$) ($P < 0.0001$, $F_{7,54} = 6.348$). (**d**) Time course of experiment showing MPEP blockade of peptidase inhibitor–induced OP-LTD (versus control, $P = 0.0037$, $t_{21} = 3.260$, $n = 14$). Representative traces are the average of the first 10 min (first of pair) and the final 5 min (second of pair) of recording. Scale bars in **d** represent 50 pA, 50 ms. Error bars in **a**,**c**,**d** indicate s.e.m. Error bars in **b** indicate the range from minimum to maximum, and box boundaries indicate 25th percentile, median and 75th percentile. Data in **a**,**b** were analyzed with Friedman test with Dunn's multiple comparisons post-test. Data in **c** were analyzed with one-way ANOVA with Dunnett's multiple comparisons post-test. Data in **d** were analyzed with unpaired Student's *t* test. $*P < 0.05$, $**P < 0.01$, $***P < 0.001$.

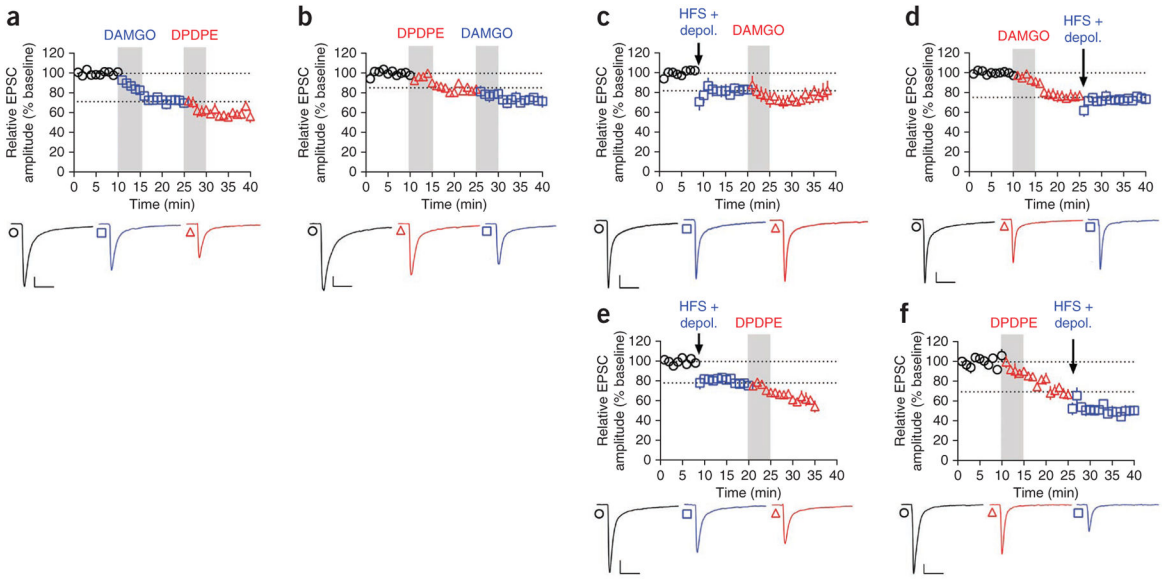

Figure 5.

mOP- and dOP-LTD operate independently. (**a**) DPDPE (0.3 μM, 5 min) induced LTD of eEPSC amplitude beyond that induced by DAMGO (0.3 μM, 5 min; versus DAMGO, P = 0.0178, t_6 = 3.237, n = 7). (**b**) DAMGO (0.3 μM, 5 min) induced LTD beyond that induced by DPDPE (0.3 μM, 5 min; versus DPDPE, P = 0.0055, t_6 = 4.222, n = 6). (**c**) eCB-LTD, induced by high-frequency stimulation (HFS, 4× 1 s at 100 Hz, 10 s apart) paired with depolarization to 0 mV, occluded LTD induced by DAMGO (0.3 μM, 5 min; versus HFS, P = 0.1121, t_7 = 1.817, n = 8). (**d**) DAMGO (0.3 μM, 5 min) occluded eCB-LTD (versus DAMGO, P = 0.5372, t_8 = 0.6447, n = 10). (**e**) eCB-LTD did not occlude LTD induced by DPDPE (0.3 μM, 5 min; versus HFS, P = 0.0013, t_6 = 5.668, n = 7). (**f**) DPDPE (0.3 μM, 5 min) did not occlude eCB-LTD (versus DPDPE, P = 0.0208, t_6 = 3.111, n = 7). Representative traces are the average of the first 10 min (first of each triplet), the 5 min before initiation of second treatment (second of each triplet), and final 5 min of recording (third of each triplet). Scale bars represent 50 pA, 50 ms. All error bars indicate s.e.m. Data in **a**–**f** were analyzed with Student's paired t tests.

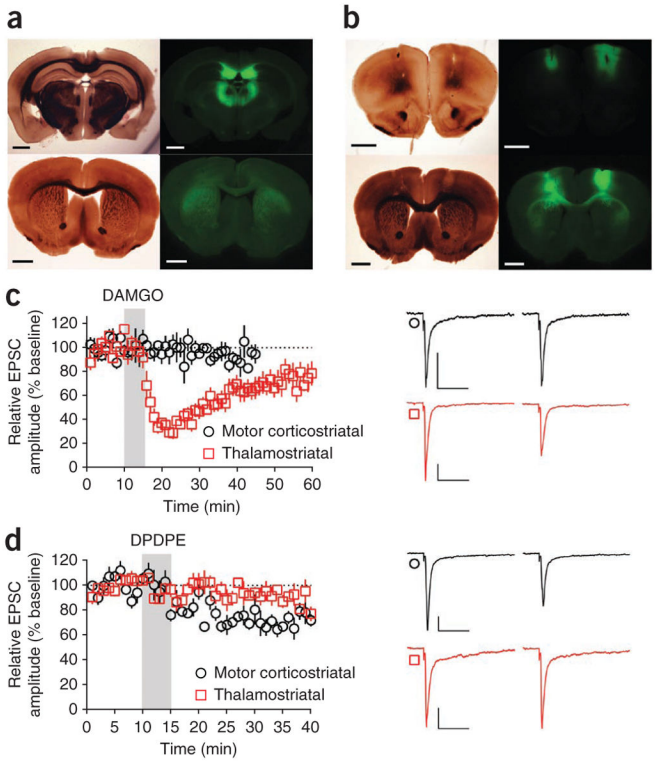

Figure 6.

MOPrs and DOPrs differentially inhibit specific striatal inputs. (**a**) Expression of ChR2-Venus in thalamic nuclei following injection of AAV vector into thalamus and expression in dorsal striatal areas receiving thalamic input. Images are representative of four injected mice. Note that thalamic injections resulted in some Venus expression in overlying hippocampus. To evaluate possible contributions of hippocampal afferents to our observations, we explicitly injected ChR2-Venus AAV vector into the hippocampus. As expected, we observed no Venus-positive afferent fibers in dorsal striatum (Supplementary Fig. 6). (**b**) Expression of ChR2-Venus in motor cortex following injection of AAV vector into M1/M2 cortices and expression in dorsal striatal areas receiving cortical input. Images are representative of six injected mice. (**c**) 470-nm light-evoked oEPSCs in DLS MSNs were greatly reduced by DAMGO (0.3 μM, 5 min) in slices in which ChR2-Venus was expressed in thalamostriatal inputs (n = 6 cells from 4 mice), and largely unchanged in slices in which ChR2-Venus was expressed in motor corticostriatal inputs (versus thalamostriatal, P = 0.0062, t_9 = 3.549, n = 5 cells from 4 mice). Thalamostriatal experiments were extended to demonstrate a continuing washout of the inhibitory effect of DAMGO. (**d**) oEPSCs in DLS MSNs were nonsignificantly inhibited by DPDPE (0.3 μM, 5 min) when ChR2-Venus was expressed in thalamostriatal inputs (n = 7 cells from 4 mice), and showed LTD following DPDPE in slices in which ChR2-Venus was expressed in motor corticostriatal inputs (versus thalamostriatal, P = 0.0022, t_{12} = 3.873, n = 7 cells from 5 mice). Scale bars in **a**,**b** represent 1 mm. Scale bars in **c**,**d** represent 50 pA, 50 ms. Representative traces are the average of the first 10 min (first of each pair) and the final 10 min (second of each pair) of recording. All error bars indicate s.e.m. Data in **c**,**d** were analyzed by unpaired Student's t test.

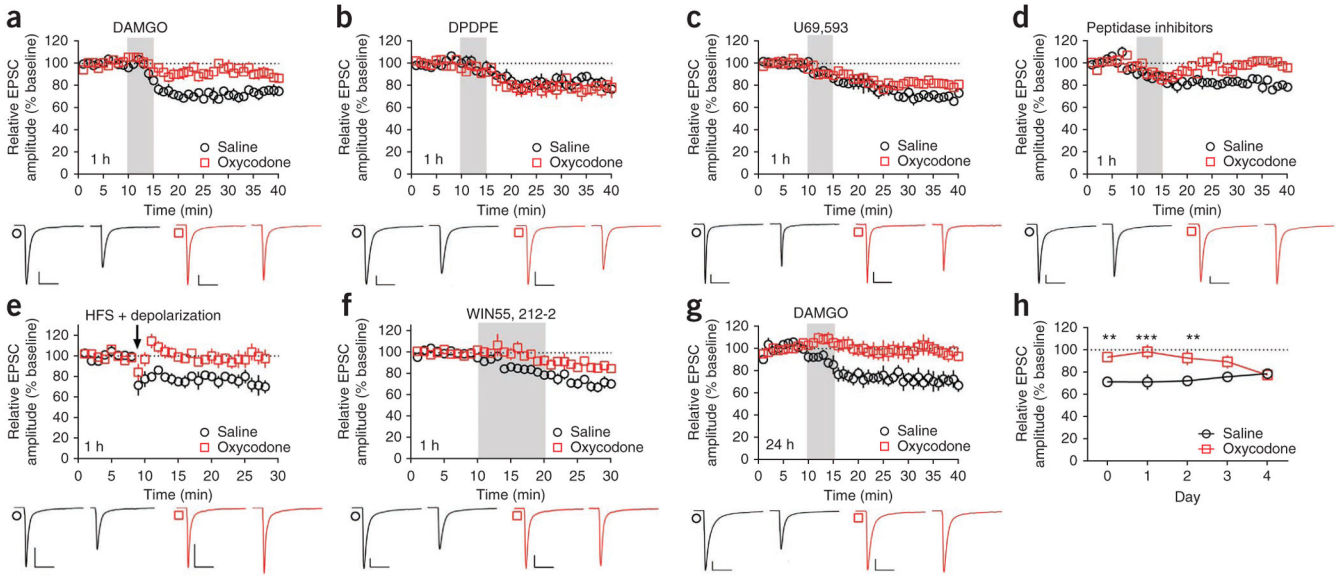

Figure 7.

A single *in vivo* exposure to oxycodone prevents induction of mOP- and eCB-LTD. (**a**) Mice injected with saline (intraperitoneal), but not oxycodone (1 mg per kg, intraperitoneal), 1 h before death showed DAMGO-induced (0.3 μM, 5 min) mOP-LTD of eEPSCs in DLS MSNs (versus saline, $P = 0.0383$, $t_4 = 3.041$, $n = 5$ mice each). (**b**) DPDPE (0.3 μM, 5 min) induced dOP-LTD in MSNs of both saline- and oxycodone-injected mice (versus saline, $P = 0.2047$, $t_4 = 1.514$, $n = 5$ mice each). (**c**) U69,593 (0.3 μM, 5 min) induced LTD in both saline- and oxycodone-injected mice and LTD was reduced in oxycodone-injected mice ($P = 0.0195$, $t_4 = 3.777$, $n = 5$ mice each). (**d**–**f**) Oxycodone disrupted LTD induced by peptidase inhibitors (5 min, versus saline, $P = 0.0029$, $t_4 = 6.499$, $n = 5$ mice each; **d**), eCB-LTD stimulation protocol ($P = 0.0147$, $t_4 = 4.116$, $n = 5$ mice each; **e**) and WIN55,212-2 application (1 μM, 10 min, $P = 0.0388$, $t_4 = 3.030$, $n = 5$ mice each; **f**). (**g**) In mice killed 24 h after an oxycodone injection, DAMGO failed to induce LTD ($P = 0.0263$, $t_5 = 3.118$, $n = 6$ mice each). (**h**) Oxycodone disrupted LTD induced by DAMGO up to 2 d post-injection. Mice were killed 1 h (day 0) to 4 d post-injection (day 0, $n = 5$ mice each; day 1, $n = 6$ mice each; day 2, $n = 6$ mice each; day 3, $n = 5$ mice each; day 4, $n = 5$ mice each; treatment: $P < 0.0001$, $F_{1,22} = 36.83$; day: $P = 0.8467$, $F_{4,22} = 0.3419$; interaction: $P = 0.0303$, $F_{4,22} = 3.265$). Representative traces are the average of the first 10 min (first of each pair) and the final 10 min (second of each pair) of recording. Scale bars represent 50 pA, 50 ms. All error bars indicate s.e.m. Data in **a**–**g** were analyzed with Student's paired *t* test. Data in **h** were analyzed with two-way repeated measures ANOVA with Sidak's multiple comparisons post-test. $^{**}P < 0.01$, $^{***}P < 0.001$.